

# Modular Process for the Flexible Synthesis of Magnetic Beads—Process and Product Validation

Birgit Hickstein,<sup>1</sup> Urs Alexander Peuker<sup>2</sup>

<sup>1</sup>Institute of Chemical Process Engineering, Clausthal University of Technology, Clausthal-Zellerfeld 38678, Germany

<sup>2</sup>TU Bergakademie Freiberg, Institut für Mechanische Verfahrenstechnik und Aufbereitungstechnik, Agricolastraße 1, Freiberg/Sachsen 09599, Germany

Received 16 May 2008; accepted 8 November 2008

DOI 10.1002/app.29655

Published online 17 February 2009 in Wiley InterScience (www.interscience.wiley.com).

**ABSTRACT:** Here we present a modular process for the flexible production of magnetic beads with variable magnetic properties and anion or cation exchanger functionalities. Magnetic beads are used in bio-separations and downstream processing to remove a valuable substance from e.g., a fermentation broth (Magnetic Fishing). The magnetic beads we are presenting here consist of a composite material, containing nanoscale magnetite and ion exchanger particles which are embedded into a polymer matrix. With this composite concept, anion and cation exchanger properties are available in magnetic beads with different matrix polymers (PVB, PVA, PMMA, and PVAc). The content of magnetite was varied in a range between 0

and 40 wt %, ion exchanger particles between 0 and 60 wt % and the matrix polymer between 20 and 60 wt %. The magnetic bead characteristics, which determine the application properties, are shown. Thermo gravimetric analyses, FTIR spectra and measurements of the ion exchange capacity prove the different properties in respect to the magnetic beads composition. In an adsorption experiment, it was possible to achieve a maximum capacity of 270 mg/g for  $\beta$ -galactosidase with PVB-beads. © 2009 Wiley Periodicals, Inc. *J Appl Polym Sci* 112: 2366–2373, 2009

**Key words:** magnetic polymers; composites; functionalization of polymers; magnetic separation; spray drying

## INTRODUCTION

Magnetic Beads are composite particles integrating magnetic and functional properties in one particle. In the literature, there is a wide range of methods for the synthesis of magnetic beads using techniques like suspension polymerization,<sup>1</sup> emulsion<sup>2,3</sup> and dispersion polymerization<sup>4</sup> or precipitation.<sup>5</sup> The size range of magnetic beads varies from 10 nm to 100  $\mu$ m. An overview about the variety of synthesis methods and size ranges is given by.<sup>6</sup>

Despite the variety of synthesis methods for magnetic beads their basic working principle is unique. On the one hand, magnetic beads are superparamagnetic, what means, that they can be separated by a magnet but are no longer magnetic when the magnet is removed. On the other hand, magnetic beads are equipped with a functional ligand being responsible for the capture of a specific target molecule. With these properties, magnetic beads can be applied in various fields where specific target molecules have to be separated from a liquid. Magnetic beads were

already applied for the isolation of cells<sup>7</sup> and the purification of plasma membranes,<sup>8</sup> for the usage in molecular applications like DNA purification<sup>9</sup> and for the removal of heavy metals from aqueous media as a potential application in wastewater treatment.<sup>10</sup> Further on Saiyed et al.<sup>11</sup> discussed their application in the field of biotechnology, biomedicine, and drug discovery. Numerous publications deal with the application of magnetic beads in protein separation. Bucak et al.<sup>12</sup> presented the successful separation of binary and ternary protein mixtures with magnetic nanoparticles. There is also experience about the application of magnetic beads in a real bioseparation process: Holschuh and Schwammle<sup>13</sup> presented a purification procedure for antibodies from a cell suspension and compared their results to the conventional purification procedure. Using the magnetic beads made them five times faster while achieving the same yield.

The wide range of possible applications of magnetic beads reveals the potential of the magnetic bead technology in industrial processes. To overcome the demands of an industrial application, magnetic beads synthesized according to the customer's separation task have to be available in large scale. Here we present a flexible synthesis procedure with a high scale-up potential for the manufacturing of magnetic beads on customers demand.

Correspondence to: B. Hickstein (hickstein@icvt.tu-clausthal.de).

Contract grant sponsor: Deutsche Forschungsgemeinschaft; contract grant number: PE 1160/3-1.

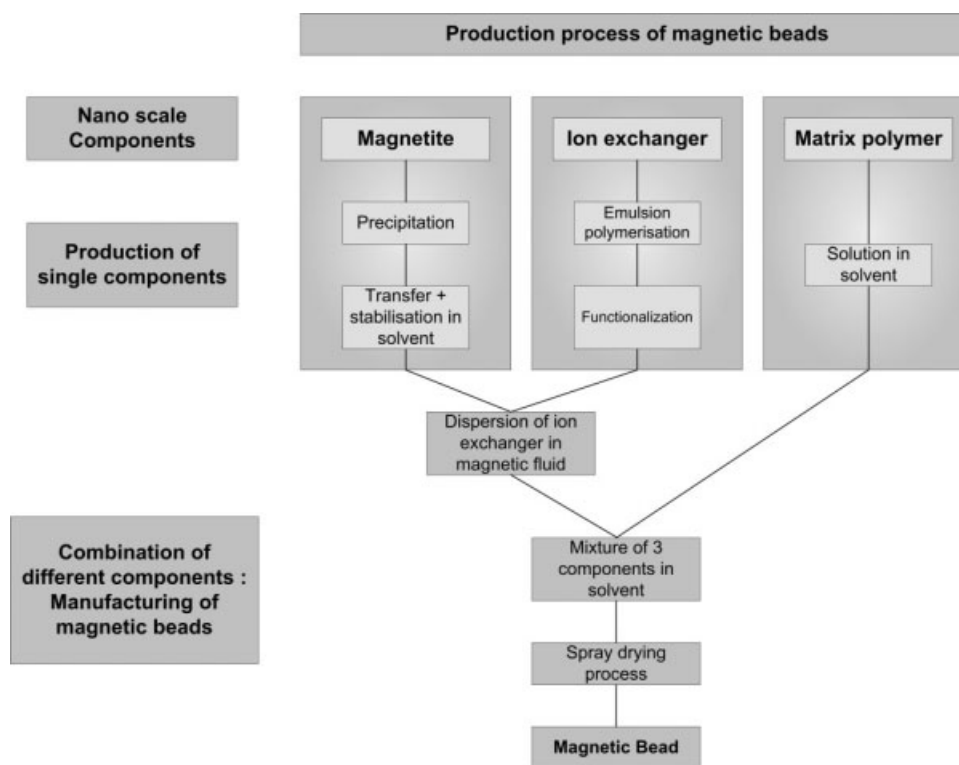


**Figure 1** Flow chart of the production process of magnetic beads.

To guarantee a flexible synthesis the process is developed in a modular design (Fig. 1). Each functionality of the magnetic beads is synthesized in an independent process. Magnetite, prepared with a precipitation process, provides the superparamagnetic properties of the magnetic beads. Nanoscale ion exchanger particles prepared by miniemulsion polymerization processes are responsible for the capture of a specific target molecule. Both components, the ion exchanger particles (anion exchanger particle AEX, cation exchanger particles CEX) and the magnetite particles, are integrated into a polymer matrix with a spray drying process. The modular conception offers the possibility to combine the different components according to the separation challenge.

Here we present the result of the flexible production process for the synthesis of magnetic beads: A high variety of magnetic beads, differing in their material combinations and compositions. The magnetic beads are characterized concerning their material properties and references are given for the successful application of the produced magnetic beads.

## EXPERIMENTAL

### Materials

We used the polymers Polyvinyl butyral (PVB: Mowital B30T powder), Polyvinyl alcohol (PVA: Mowiol 4-88), Polymethyl methacrylate (PMMA), and Polyvinyl acetate (PVAc) as matrix polymers. PVB and PVA

were obtained from Kuraray Specialities Europe (KSE) [Frankfurt, Germany], PMMA was from Lucite International (Southampton, United Kingdom) and PVAc was from Wacker (München, Germany).

For the synthesis of the magnetic fluids ( $\text{Fe}_3\text{O}_4$  in DCM and in water) we used the following substances from Sigma Aldrich: oleic acid ( $\text{C}_{18}\text{H}_{34}\text{O}_2$ ), iron(II)sulfate heptahydrate ( $\text{FeSO}_4 \cdot 7\text{H}_2\text{O}$ ) and iron(III)chloride hexahydrate ( $\text{FeCl}_3 \cdot 6\text{H}_2\text{O}$ ), dichloromethane (DCM), sodium hydroxide (NaOH) and ammonium hydroxide (26%  $\text{NH}_3$ ). PVA was the same as aforementioned.

Nanoscale anion and cation exchanger particles were produced with a miniemulsion polymerization with the following materials: chloroform, hexadecane, chlorosulfuric acid, toluene, vinylbenzyl chloride (VBC) and styrene from Fluka, divinylbenzene (DVB) and peroxodisulfate ( $\text{Na}_2\text{S}_2\text{O}_8$ ) from Merck (Darmstadt, Germany) and sodium dodecylsulfate (SDS) from Sigma Aldrich (Taufkirchen, Germany). Trimethylamine was delivered by GHC (Gerling, Holz & Co.), (Hamburg, Germany). Petroleum ether that was used within the synthesis procedure of the beads was also from Fluka.

The adsorption experiments were conducted with  $\beta$ -galactosidase (G5160) from Sigma Aldrich (Taufkirchen, Germany). Therefore, we prepared a buffer from potassium dihydrogen phosphate ( $\text{KH}_2\text{PO}_4$ ) and di-potassium hydrogen phosphate ( $\text{K}_2\text{HPO}_4$ ) purchased from Merck, (Darmstadt, Germany). Enzyme concentration was determined with Total

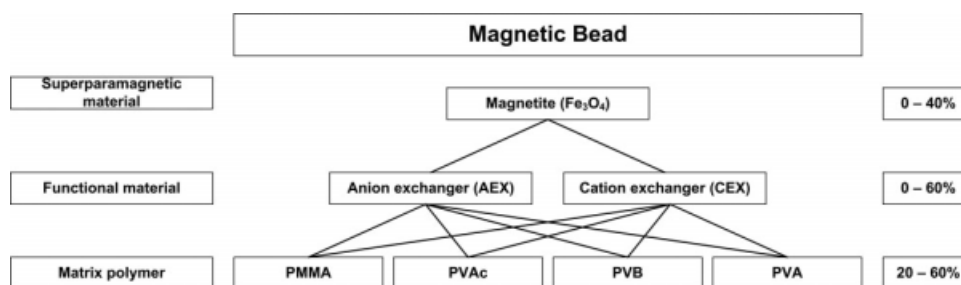


Figure 2 Flow chart of the various combinatorial possibilities for the production of magnetic beads.

Protein Kit, Micro-Lowry (RP0300-1KT) from Sigma Aldrich (Taufkirchen, Germany).

### Magnetic beads

The magnetic beads are prepared from magnetite nanoparticles, nano ion exchanger particles, and different matrix polymers. The combinatorial possibilities for the composition of magnetic beads are shown in Figure 2. Each single component ( $\text{Fe}_3\text{O}_4$ , AEX, CEX) is synthesized in an independent, scaleable process. The magnetic beads are produced via a spray drying process with spray dryer from Büchi Labortechnik (Büchi B191, Büchi Labortechnik GmbH, Germany).

Details of the synthesis processes of magnetite, AEX and CEX as well as the spray drying process are given in the following publications: An organic magnetic fluid on the basis of magnetite nanoparticles with an average particle size of 5–10 nm is synthesized by a magnetite precipitation followed by a transfer in DCM.<sup>14</sup> Oleic acid with a concentration of 0.2 g oleic acid/g  $\text{Fe}_3\text{O}_4$  serves as a surfactant to stabilize the magnetite nanoparticles in DCM. An aqueous magnetic fluid with PVA as the stabilizer for the magnetite nanoparticles was manufactured according to.<sup>5</sup> The AEX particles consist of a VBC-DVB copolymer with a quaternary ammonium group as an anion exchanger ligand, the CEX particles are made up of a PS-DVB copolymer with a sulfuric group as a cation exchanger ligand. Both particle systems, the PS-DVB and the VBC-DVB particles, show an average particle size of 160–260 nm. They were manufactured by a miniemulsion polymerization according to.<sup>15</sup> Details of the manufacturing procedure of the AEX and CEX particles and the process variables of the spray-drying process are given elsewhere.<sup>16,17</sup> For the manufacturing of the PVB, PVAc and the PMMA beads we used DCM as the solvent and the DCM based magnetic fluid for the delivering of magnetite. For the manufacturing of PVA beads water served as the solvent in combination with the aqueous based magnetic fluid.

The produced magnetic beads are composed of one matrix polymer, a variable magnetite content and different amounts of AEX or CEX particles. Within the spray-

drying process the nanoparticles are embedded into the matrix polymer. The results are magnetic beads with cation or anion exchanger functionalities with different matrix polymers and different magnetite contents.

To distinguish between the different variations we use the following nomenclature for the description of the bead's composition (related to the weight percentage): matrix polymer/magnetite/ion exchanger. A bead with the specification "PMMA-bead 50/30/20 with AEX" consists of 50 wt % PMMA, 30 wt % magnetite and 20 wt % AEX particles.

### Analysis and measurements

To determine the different quantities of the single magnetic bead properties the produced beads were characterized with the following methods: Scanning electron microscopy<sup>18</sup> pictures were taken to analyze the surface and the morphology of the magnetic beads. Additional surface measurements according to Brunauer, Emmert, and Teller (BET) were conducted. The particle sizes were measured with a laser diffraction spectrometer. Alternating gradient magnetometer (AGM) measurements revealed the magnetic properties in dependence from the magnetite content of the beads and thermo gravimetric analysis (TGA) served to control the magnetite content. Different contents of AEX and CEX were verified with the help of Fourier Transform infrared spectrometry (FTIR) taken with the Photoacoustic spectroscopy (PAS) technology and with measurements of the ion exchange capacity of the beads with a titration according to.<sup>19</sup> The capacity of the beads concerning their adsorption properties of proteins were analyzed by taking an adsorption isotherm with  $\beta$ -galactosidase. Protein concentrations were measured with the Lowry test. The adsorption experiments were conducted in a  $\text{K}_2\text{HPO}_4/\text{KH}_2\text{PO}_4$  buffer with a pH of 4, desorption was done while changing the pH to 8. Magnetic beads were applied with a concentration of 1 mg/mL for 1 h in both experiments. Maximal capacity  $Q_m$  was calculated while using the Langmuir model to describe the adsorption of the protein to the beads. The Langmuir model is described elsewhere.<sup>20,21</sup>

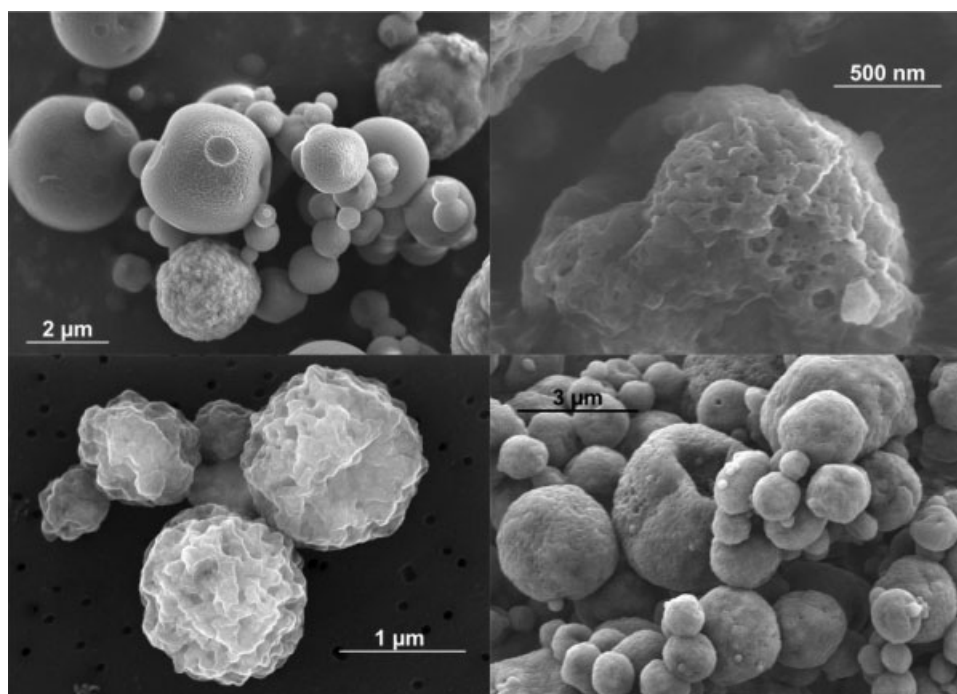


**Figure 3** SEM pictures from magnetic beads. Clockwise starting from the left corner: PVA-beads 50/20/30 with CEX, PMMA-beads 40/20/40 with CEX, PVB-beads 40/20/40 with CEX and PVB-beads 40/20/40 with AEX.

## RESULTS AND DISCUSSION

Figure 3 shows SEM pictures of magnetic beads made from PVA, PMMA, and PVB. The surface of PVA-beads is relatively smooth in contrast to the other materials. PMMA-beads show the roughest surface. These observations are underlined by BET measurements: PMMA-beads showed a surface of  $9.55 \text{ m}^2/\text{g}$ , PVB-beads with the same composition (60/20/20 with CEX) had a surface of  $3.92 \text{ m}^2/\text{g}$  (Table I). In accordance to their very smooth surface PVA-beads show the lowest surface. As the BET-surfaces of the different materials are distributed in the same magnitude the different porosities just originate from dissimilar morphologies e.g., roughness of the polymers but not from any inner porosity. From the SEM pictures the particle sizes are distributed between  $500 \text{ nm}$  and  $3 \mu\text{m}$ , particle size measurements reveal a negligible broader distribution (Fig. 4).

The results of TGA analysis of PMMA-beads with a constant content of 20 wt % CEX and variable con-

tent of magnetite (10–40 wt %) and PMMA (70–40 wt %) is shown in Figure 5. The beads were washed with petroleum ether to remove adhered particles that were not integrated into the beads. TGA analysis of the pure components PMMA and CEX showed, that these materials totally decompose while heating up to  $700^\circ\text{C}$  whereas, magnetite is not decomposed (data not presented). Thus the remaining mass can be allocated to the mass fraction of magnetite. It increases linear with an increasing content of magnetite. The analyses were repeated with unwashed beads. The results of both analyses (TGA

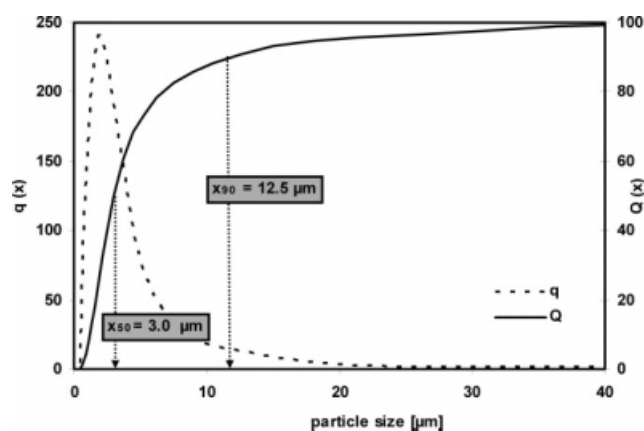


**Figure 4** Particle size distribution of PMMA-beads 50/30/20 CEX; straight line represents the cummulation curve  $[Q(x)]$ ; dashed line is the frequency distribution  $[q(x)]$ .

**TABLE I**  
BET Surfaces of Magnetic Beads

Sample	Surface ( $\text{m}^2/\text{g}$ )
PMMA 60/20/20 CEX	9.55
PMMA 40/20/40 AEX	7.07
PVB 60/20/20 CEX	3.92
PVB 40/20/40 CEX	3.45
PVA 50/30/20 CEX	1.57



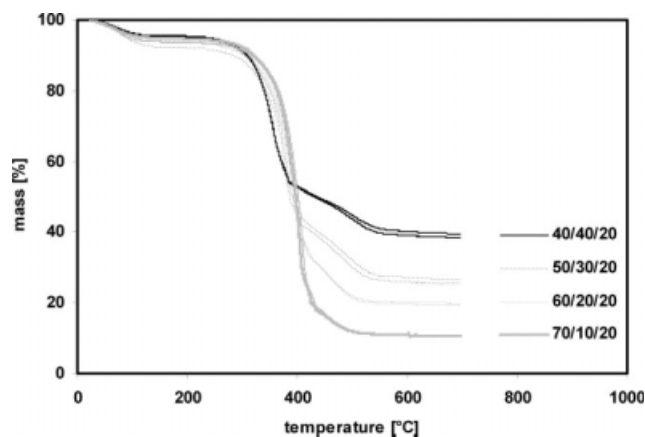


**Figure 5** TGA analysis of washed PMMA-beads with 20 wt % CEX and various contents of magnetite/matrix polymer. Parameters of TGA-analysis: Heating rate: 20°C/min, gas: 80% N<sub>2</sub> and 20% O<sub>2</sub>.

of washed and unwashed beads) are summarized in Table II. There is no significant difference between washed and unwashed beads observable. From the last fact we can conclude, that magnetite is totally embedded into the magnetic beads even at high filling degrees.

The magnetic properties of the same PMMA-beads shown in Figure 5 were analyzed with AGM. The results are presented in Figure 6. The progress of the magnetization curve of sample PMMA 40/40/20 CEX demonstrates exemplarily the superparamagnetic behavior. The magnetic saturation increases with the magnetite content. The increase of the magnetic saturation is as linear as the increase of the magnetite fraction shown in Figure 5. Just the sample 50/30/20 shows discrepancies from the linear increase while considering the AGM measurements as well as the TGA analysis. As this deviation emerges in both analyses, the reason is probably an incorrect dosage of the magnetite content in the production process of the magnetic beads. The magnetic remanence of the beads is very weak. The magnetic properties are summarized for the PMMA-beads and for three additional beads in Table III. All magnetic

**TABLE II**  
Comparison of Magnetite Content Between Washed and Unwashed Beads

Sample	Remaining magnetite content in mass (%)	
	Beads unwashed	Beads washed
70/10/20	10.84	10.70
60/20/20	19.40	19.56
50/30/20	27.94	26.02
40/40/20	39.07	38.92

Results originate from TGA analysis.

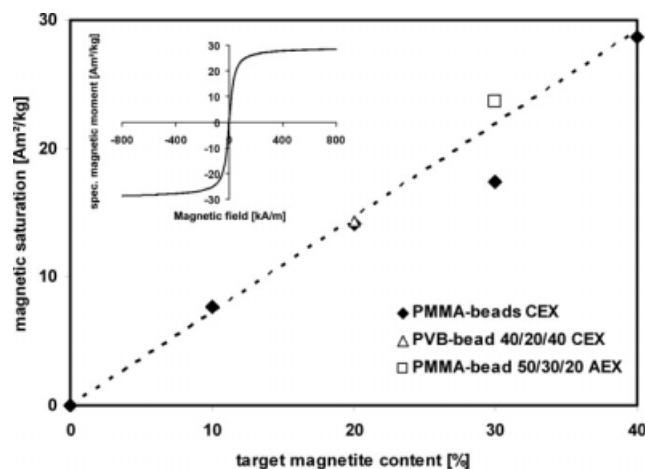


**Figure 6** Magnetization curve of sample PMMA 40/40/20 CEX and magnetic saturation of magnetic beads in dependence from the target magnetite content. PMMA-beads (◆) contain a fixed content of 20 wt % CEX and a variable magnetite content of 10–40 wt %. The dotted line represents the ideal progression. Results originate from AGM analysis as presented in the small diagram.

beads except one sample were manufactured with the organic magnetic fluid, sample PVA 50/20/30 CEX was manufactured with the aqueous magnetic fluid. Relating the magnetic saturation to the content of magnetite, the average magnetic saturation of the organic magnetic fluid based beads is, without considering sample PMMA 50/30/20 CEX, 73.9 Am<sup>2</sup>/kg Fe<sub>3</sub>O<sub>4</sub>. The corresponding magnetic saturation of the aqueous based magnetic bead PVA 50/20/30 CEX is 50.8 Am<sup>2</sup>/kg Fe<sub>3</sub>O<sub>4</sub>. A control measurement of the pure, spray dried magnetite particles that originated from the aqueous magnetic fluid, showed a magnetic saturation of 50.4 Am<sup>2</sup>/kg. This value fits very well to the values given by the authors of the synthesis process of the aqueous magnetic fluid, which range between 46.6–56.1 Am<sup>2</sup>/kg in dependence from the surfactant concentration.<sup>5</sup> The higher magnetic saturation of the magnetic material originating from the organic magnetic fluid may be explained by a better stabilization of the nanoscale magnetite particles by the surfactant oleic acid. As the magnetic saturation depends on the particle size of the superparamagnetic material a better stabilization may lead to smaller particles resulting in higher magnetic saturation values. In literature, the magnetic saturation of Fe<sub>3</sub>O<sub>4</sub> particles range from 30 to 90 Am<sup>2</sup>/kg depending on the synthesis method.<sup>3,22–24</sup>

The content of AEX particles in the magnetic beads was controlled by analyzing the beads with the FTIR technique and via measurements of the ion exchange capacity. FTIR spectra were taken from PVB-beads with a fixed magnetite content of 20 wt %.

**TABLE III**  
Magnetic Saturation ( $M_s$ ) and Magnetic Remanence ( $M_r$ ) of Magnetic Beads

Sample	$M_s$ (Am <sup>2</sup> /kg)	$M_r$ (Am <sup>2</sup> /kg)	$M_r/M_s$	$M_s$ (Am <sup>2</sup> /kg Fe <sub>3</sub> O <sub>4</sub> )
PMMA 40/40/20 CEX	28.68	0.234	0.0082	71.7
PMMA 50/30/20 CEX	17.38	0.085	0.0049	57.9
PMMA 60/20/20 CEX	14.12	0.097	0.0069	70.6
PMMA 70/10/20 CEX	7.67	0.072	0.0094	76.7
PVB 40/20/40 CEX	14.38	0.074	0.0052	71.9
PMMA 50/30/20 AEX	23.61	0.189	0.0080	78.7
PVA 50/20/30 CEX	10.16	0.081	0.0080	50.8

All sample except the last one were manufactured with an organic magnetic fluid, sample PVA 50/20/30 CEX was manufactured with an aqueous-based magnetic fluid.

The content of AEX particles was 20, 40, and 60 wt %, the according content of PVB was 60, 40, and 20 wt %. Spectra were also taken from pure PVB and AEX. Figure 7 shows in a section of the spectra the enhancement of the PVB bands with an increase of the PVB-content, Figure 8 shows the same effect while considering the AEX band. Both figures originate from the same spectra from the same PVB-beads.

The Tables IV–VI contain the ion exchange capacities of various beads determined via the titration method. Table IV includes results for magnetic beads without CEX or AEX particles. These values can be considered as the blank for the beads as well as for the measurement method. The predominant contribution to the CEX blank values may originate from the matrix polymers. This assumption is reasonable as the CEX activity decreases with a reduction of hydroxide groups as the main H<sup>+</sup> exchanging group in the matrix polymer. The blank AEX activity of the polymer/magnetite beads ranges

within such low values that these results may be allocated to the blank value of the measurement method. As the contribution of the matrix polymer to the CEX activity is relatively high we subtracted the blank CEX activity from the initial ion exchange activity of the CEX containing beads. The results of these calculations are the corrected activities shown in Table V. Table VI includes the anion exchange activities of different beads with AEX particles. Because of the very low blank values of the corresponding blank beads these data were not corrected.

The high contribution of the matrix material to the CEX activities indicates, that not every polymer is suitable for the production of magnetic particles with CEX function. Otherwise, the contribution of the matrix polymer ion exchange activity to the capacity of the real adsorption process has to be checked experimentally for the particular target molecule.

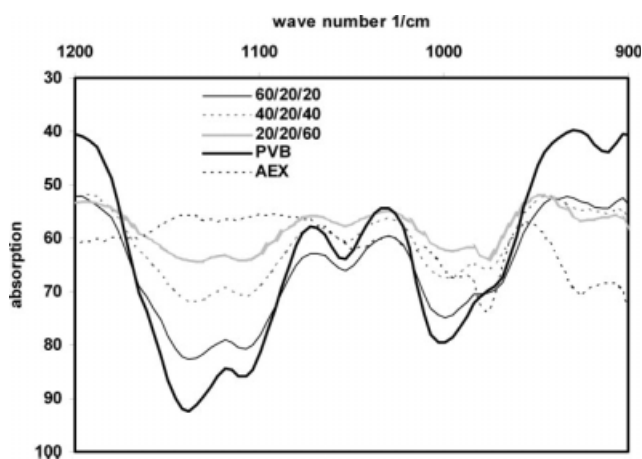


**Figure 7** FTIR-spectra of PVB-beads with a fixed content of magnetite (20 wt %), variable contents of PVB (20–60 wt %) and variable contents of AEX (20–60 wt %). The spectra PVB and AEX were taken from the pure raw material. The figure shows the increase of the PVB-related bands with an increasing PVB-content of the beads.

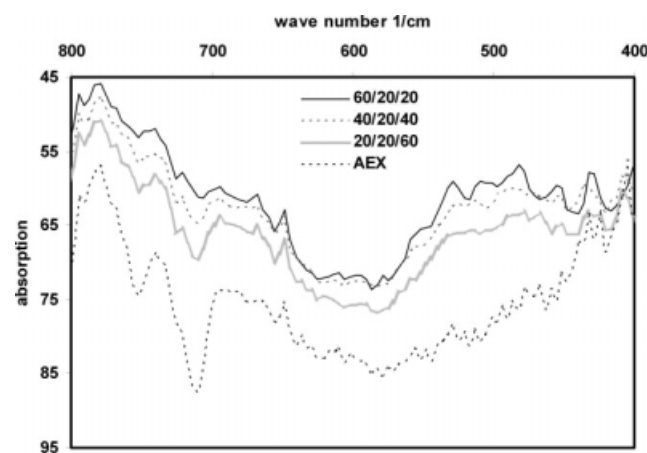


**Figure 8** FTIR-spectra of PVB-beads with a fixed content of magnetite (20 wt %), variable contents of PVB (20–60 wt %) and variable contents of AEX (20–60 wt %). The spectra PVB and AEX were taken from the pure raw material. The figure shows the increase of the AEX-related bands with an increasing AEX-content of the beads. The bands of the AEX particles can be referred to the functional amino group of the AEX particles.

**TABLE IV**  
Ion Exchange Capacities of Polymer Beads with 20 wt % Magnetite ("Blank Activity" of 80/20/00 Beads)

Polymer	Blank activities (mval/g)	
	CEX	AEX
PVA	2.09	
PVB	0.51	0.028
PMMA	0.32	0.035
PVAc		0.027

The capacity of the magnetic beads concerning the adsorption of proteins was determined in an adsorption experiment with  $\beta$ -galactosidase. Therefore, PVB-beads with a magnetite content of 20 wt % and a CEX content of 20 and 40 wt % were used (Fig. 9). On average, it was possible to remove 30.8% of the initial protein concentration with the 40/20/40 beads and 10.5% with the 60/20/20 beads. In a desorption experiment with the 40/20/40 beads we achieved an average desorption rate of 85.8% related to the adsorbed protein. There was no loss of activity of the protein observable.

Further on we tested the application of the magnetic beads in various fields: They were successfully applied in a solid phase support synthesis,<sup>25</sup> we characterized their potential in protein separation<sup>16,17</sup> and magnetic beads were used for the production of superparamagnetic assemblies via the further processing of magnetic beads with an extruder.<sup>26</sup> Beyond these applications the utilization of the pure nanoscale AEX and CEX particles in filter materials becomes possible.

## CONCLUSION

Here we present a modular process for the flexible manufacturing of magnetic beads. With this process we are able to combine four different matrix polymers with two different functionalities together with superparamagnetic magnetite. The quantitative com-

**TABLE V**  
Corrected Cation Exchange Activities of PVB and PMMA Beads with CEX and 20% Magnetite

Content CEX (%)	Corrected activity with different matrix polymer (mval/g)		Content polymer (%)
	PVB	PMMA	
10	0.50	0.45	70
20	0.94	1.24	60
30	1.52	1.17	50
40	1.83	1.98	40
50	2.08	2.50	30
100		4.58	0

**TABLE VI**  
Anion Exchange Capacities of Different Beads with AEX Particles (Noncorrected Data)

Content AEX (%)	Activity with different matrix polymer (mval/g)			Content polymer (%)
	PVB	PMMA	PVAc	
20	0.33	0.38	0.23	60
40	0.98	0.76	0.50	40
60	1.41	0.82	1.00	20
100		1.80		0

position of the beads is very flexible. The magnetite content determines the maximum magnetic saturation, the kind of ion exchanger nanoparticles characterizes the functionality and the matrix polymer defines the morphology, the surface structure and the wettability of the magnetic beads in a solvent. Thus, we are able to produce several charges of magnetic beads with a high variety of different properties. As every single process step is easy for a scale-up the production of magnetic beads in large scale becomes possible with this process.

To expand the capabilities of the beads for further applications the development of further functional ligands becomes necessary. Therefore, the integration of metal affinity ligands or the attachment of Protein A is imaginable. Moreover we need to characterize the different magnetic beads as well as their basic components, the AEX and CEX, in detail. In the future, these characterizations will help to predict how a magnetic bead has to be composed to fulfill a certain separation problem. In a characterization process high amounts of experiments have to be conducted whereby the implementation of high-throughput experiments becomes necessary.

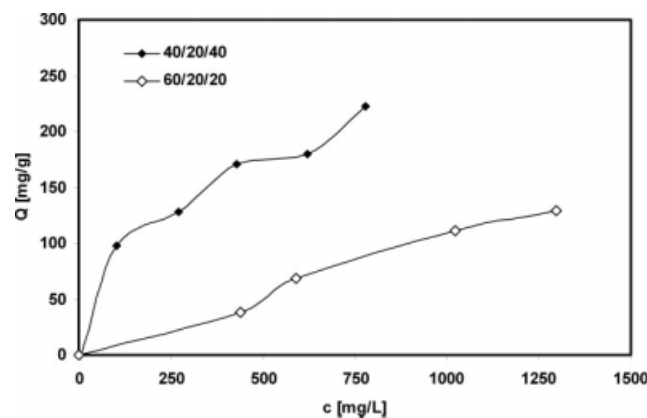


**Figure 9** Adsorption of  $\beta$ -galactosidase on PVB-beads with a fixed magnetite content of 20 wt % and a CEX content of 20 and 40 wt %. Adsorption was done at pH 4. Maximal capacity  $Q_m$  calculated according to Langmuir is 270 mg/g for the 40/20/40 beads.

The authors thank Dr. Franzreb, Forschungszentrum Karlsruhe (Karlsruhe, Germany), for analyzing the magnetic properties of the magnetic beads.

### NOMENCLATURE

AEX	Anion exchanger
AGM	Alternating gradient magnetometer
BET	Method developed by Brauner, Emmet and Teller for the determination of particle surfaces
$c$	Equilibrium concentration (mg/L)
CEX	Cation exchanger
DVB	Divinylbenzene
DCM	Dichloromethane
FTIR	Fourier transform infrared spectroscopy
$M_r$	Magnetic remanence ( $\text{Am}^2/\text{kg}$ )
$M_s$	Magnetic saturation ( $\text{Am}^2/\text{kg}$ )
mval/g	Ion exchange activity unit
$Q$	Equilibrium capacity (mg/g)
$Q_m$	Maximal capacity (mg/g)
PAS	Photoacoustic technology
PMMA	Polymethyl methacrylate
PS	Polystyrene
PVA	Polyvinyl alcohol
PVAc	Polyvinyl acetate
PVB	Polyvinyl butyral
SDS	Sodium dodecylsulfate
SEM	Scanning electron microscopy
TGA	Thermo gravimetric analysis
wt %	weight percent

### References

- Cocker, T. M.; Fee, C. J.; Evans, R. A. *Biotechnol Bioeng* 1997, 53, 79.
- Yang, S.; Liu, H. R.; Zhang, Z. C. *J Polym Sci Part A: Polym Chem* 2008, 46, 3900.
- Ramirez, L. P.; Landfester, K. *Macromol Chem Phys* 2003, 204, 22.
- Horak, D.; Benedyk, N. *J Polym Sci Part A: Polym Chem* 2004, 42, 5827.
- Lee, J.; Isobe, T.; Senna, M. *J Colloid Interface Sci* 1996, 177, 490.
- Yuan, Q.; Williams, R. A. *China Particuol* 2007, 5, 26.
- Safarik, I.; Safarikova, M. *J Chromatogr B* 1999, 722, 33.
- Lawson, E. L.; Clifton, J. G.; Huang, F. L.; Li, X. S.; Hixson, D. C.; Josic, D. *Electrophoresis* 2006, 27, 2747.
- Uhlen, M. *Nature* 1989, 340, 733.
- Denizli, A.; Tanyolac, D.; Salih, B.; Ozdural, A. *J Chromatogr A* 1998, 793, 47.
- Saiyed, Z. M.; Telang, S. D.; Ramchand, C. N. *Biomagn Res Technol* 2003, 1.
- Bucak, S.; Jones, D. A.; Laibinis, P. E.; Hatton, T. A. *Biotechnol Prog* 2003, 19, 477.
- Holschuh, K.; Schwammle, A. *J Magn Magn Mater* 2005, 293, 345.
- Banert, T.; Peuker, U. A. *J Mater Sci* 2006, 41, 3051.
- Landfester, K. *Adv Mater* 2001, 13, 765.
- Hickstein, B.; Peuker, U. A. *Biotechnol Prog* 2008, 24, 409.
- Käppler, T. E.; Hickstein, B.; Peuker, U. A.; Posten, C. *J Biosci Bioeng* 2008, 105, 579.
- Thode, K.; Luck, M.; Semmler, W.; Muller, R. H.; Kresse, M. *Pharm Res* 1997, 14, 905.
- Lux, H. *Praktikum der Quantitativen Anorganischen Analyse*; Verlag von H.F. Bergman: München, Germany, 1967.
- Yang, C. L.; Liu, H. Z.; Guan, Y. P.; Xing, J. M.; Liu, J. G.; Shan, G. B. *J Magn Magn Mater* 2005, 293, 187.
- Tong, X. D.; Xue, B.; Sun, Y. *Biotechnol Prog* 2001, 17, 134.
- Lu, A. H.; Salabas, E. L.; Schüth, F. *Angew Chem* 2007, 119, 1242.
- Guan, Y. P. *Synthesis, characterization and applications of superparamagnetic polymer nanostructured carriers for affinity separation*, PhD thesis, IPE CAS, Beijing, 2000.
- Reddy, K. R.; Lee, K. P.; Gopalan, A. Y.; Kang, H. D. *React Funct Polym* 2007, 67, 943.
- Hickstein, B.; Cecilia, R.; Kirschning, A.; Kunz, U.; Peuker, U. A. *Chem Ing Tech* 2007, 79, 2089.
- Banert, T.; Peuker, U. A. *Chem Ing Tech* 2005, 77, 1232.